Biochemical and Biophysical Research Communications 433 (2013) 276–280

Contents lists available at SciVerse ScienceDirect

Biochemical and Biophysical Research Communications

journal homepage: www.elsevier.com/locate/ybbrc

Peptide concentration alters intermediate species in amyloid β fibrillation kinetics

M. Garvey [1], I. Morgado *

Max-Planck Research Unit for Enzymology of Protein Folding, Weinbergweg 22, 06120 Halle (Saale), Germany

ARTICLE INFO

Article history:
Received 2 February 2013
Available online 26 February 2013

Keywords:
Amyloid β
Aggregation
Concentration
Nucleation
Sodium phosphate

ABSTRACT

The kinetic mechanism of amyloid aggregation remains to be fully understood. Investigations into the species present in the different kinetic phases can assist our comprehension of amyloid diseases and further our understanding of the mechanism behind amyloid β (Aβ) (1–40) peptide aggregation. Thioflavin T (ThT) fluorescence and transmission electron microscopy (TEM) have been used in combination to monitor Aβ(1–40) aggregation *in vitro* at both normal and higher than standard concentrations. The observed fibrillation behaviour deviates, in several respects, from standard concepts of the nucleation–polymerisation models and shows such features as concentration-dependent non-linear effects in the assembly mechanism. Aβ(1–40) fibrillation kinetics do not always follow conventional kinetic mechanisms and, specifically at high concentrations, intermediate structures become populated and secondary processes may further modify the fibrillation mechanism.

1. Introduction

Amyloid fibril formation, initiating from amyloid β (Aβ) peptide, is a nucleation-dependent reaction which consists of lag and growth phases [1]. These phases are thought to reflect the fibril nucleation reaction and the exponential growth of amyloid fibrils from these nuclei (respectively) [2]. Both stages are known to be affected by factors such as environment, sample concentration and secondary reaction processes, e.g. fibril fragmentation [3]. Kinetic analyses of fibril formation are frequently based on bulk spectroscopic methods, such as binding of the fibril-specific fluorescent dye thioflavin T (ThT), while particle shape and size distributions can be analysed using single-particle measurements, like electron microscopy (EM) [2]. For Aβ(1–40) peptide, different aggregates are known to arise over the course of assembly, from micelle-like oligomers to small-sized protofibrils and mature polymorphic fibrils [4]. These species can be differentiated by their morphologies, with oligomers often spherical in nature, protofibrils thin in diameter (6–10 nm), curvilinear and usually under 100 nm in length, and mature fibrils generally several μm long, greater than 10 nm in diameter and of straight morphology [5]. Using a combination of ThT and TEM, we here demonstrate non-linear features in the kinetics of Aβ fibril formation, revealing that intermediate populations may play significant roles in the development of final amyloid fibril structures.

2. Materials and methods

2.1. Expression of Aβ peptide

Aβ(1–40) was prepared by in house recombinant expression according to published procedures [6].

2.2. Kinetic analyses using ThT fluorescence

Bulk fibrillation kinetics measurements were carried out with Aβ(1–40) peptide in 50 mM HEPES buffer, pH 7.4. Fibril formation was monitored by using the ThT method and peptide concentrations ranging from 5 to 250 μM. All measurements used thoroughly disaggregated peptide. Measurements were carried out concurrently and in a parallelized assay format, which uses 96-well plates to allow semi-high throughput analyses. Each sample was measured with 8 replicates to account for the known variability of such reactions [7]. Aβ(1–40) samples at each concentration were incubated at 37 °C in 50 mM HEPES or sodium phosphate buffer pH 7.4 with 20 μM ThT, 5% dimethyl sulfoxide and 10 mM sodium azide. Errors are standard error of the mean.

2.3. Analysis of Aβ fibrils by transmission electron microscopy

Negative stain TEM-specimens were prepared as described [6] from samples taken throughout the ThT kinetic analysis. Briefly, at time-points of 0, 1, 6, 11 and 86 h the FLOUstar reader was

* Corresponding author. Present address: Centre of Marine Sciences, University of Algarve, Campus de Gambelas 8000-139, Faro, Portugal.
E-mail addresses: megan.garvey@molbiotech.rwth-aachen.de (M. Garvey), immorgado@ualg.pt (I. Morgado).
[1] Present address: Institute for Molecular Biotechnology, RWTH Aachen University, Worringerweg 1, 52074 Aachen, Germany.

0006-291X/$ - see front matter © 2013 Elsevier Inc. All rights reserved.
http://dx.doi.org/10.1016/j.bbrc.2013.02.073

paused, a 10 μL aliquot removed from an un-sampled well (for each concentration) and the reader restarted within a 4 min window. TEM images were obtained using a Zeiss CEM 902A electron microscope operated at an accelerating voltage of 80 kV. ImageJ software (http://imagej.nih.gov/ij/) was used for fibril counting (100 particles from 3 to 5 images/sample). Errors are standard error of the mean.

3. Results

We set out to examine the aggregation of recombinantly expressed Aβ(1–40) peptide [6] over a range of concentrations, using time-resolved ThT fluorescence spectroscopy [6]. At 5–50 μM Aβ(1–40) in 50 mM HEPES pH 7.4 (37 °C), we observed conventional kinetic behaviour with well-resolved lag and growth phases (Fig. 1A). At 50 μM the lag phase, t_l, was 24.9 ± 4.1 h with very low fluorescence readings. Lower Aβ concentrations led as expected to increased t_l values, and thus a longer lag time (Fig. 1B). Reducing the Aβ concentration also altered the growth phase, denoted by k [8], the apparent rate constant of fibril growth (Fig. 1C). Thus, Aβ kinetics at these concentrations were concentration dependent and in agreement with standard kinetic theory.

By contrast, higher peptide concentrations exhibited non-standard kinetic characteristics. For these samples it was difficult to define a normal lag phase. The fluorescence readings were clearly non-zero within the first 24 h (Fig. 1A), after which a further fluorescence increase occurs similar to the growth phase seen for the 50 μM sample. In our samples, at ⩾100 μM Aβ, we used this late fluorescence increase to define both k and the length of t_l. Despite the higher concentrations of these samples, t_l is approximately equivalent to the 50 μM Aβ sample (Fig. 1B). Further, we found that the k values from samples at ⩾100 μM concentration were smaller (<0.2 h^{-1}) than those obtained at 50 μM (Fig. 1C), in direct contrast to canonical behaviour [9]. We find that similar concentration-dependent kinetic properties with Aβ(1–40) occurred in 50 mM sodium phosphate buffer, pH 7.4 (Fig. 1D) as for HEPES, indicating that the non-standard kinetic effects are independent from the buffer system.

The early reaction step at high Aβ concentrations, i.e. the marked initial fluorescence increase (Fig. 1), indicates the formation of an intermediate Aβ species. We analysed samples formed

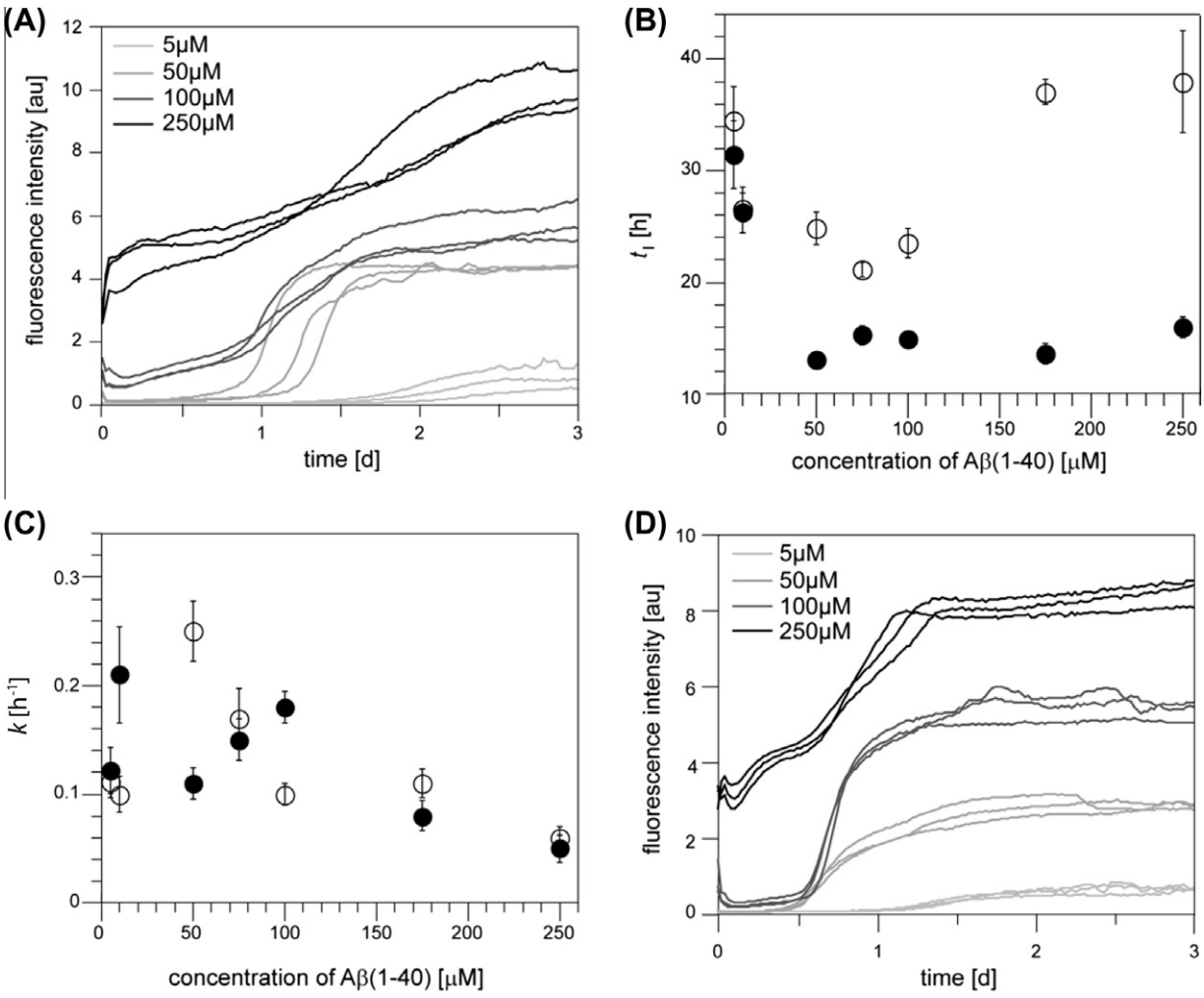

Fig. 1. Concentration effects on the aggregation of Aβ(1–40). (A) ThT fluorescence intensity of Aβ(1–40) in 50 mM HEPES buffer, pH 7.4 at 37 °C (concentrations as shown in the Figure key, 3 replicates per concentration). (B) t_l of Aβ(1–40) in HEPES (open circles) and phosphate (closed circles) buffers, both 50 mM, pH 7.4. At concentrations of 100 μM and above, t_l was determined to be complete at the start of the final growth phase. (C) k of Aβ(1–40) in HEPES (open circles) and phosphate (closed circles) buffers, both 50 mM, pH 7.4. At concentrations of 100 μM and above, k was determined to constitute the final growth phase. (D) ThT fluorescence intensity of Aβ(1–40) in 50 mM sodium phosphate, pH 7.4 (concentrations as shown in the Figure key, three replicates per concentration). For panels (B) and (C) error bars show standard error of the mean for 8 replicates.

in HEPES at different time-points and concentrations with a single-particle technique (EM) [6]. At the earliest tested time point (1 h) all samples contained a meshwork of non-fibrillar or nascently protofibrillar structures (Fig. 2).

Surprisingly, at 6 h all samples contained significant quantities of fibrils, with the fibril yield increasing with concentration (Fig. 2). Due to the morphological fibril characteristics (straight shape, fibril widths of ~11 nm or greater and fibril lengths >100 nm; Fig. 3), these were classified as mature amyloid fibrils. In addition, some non-fibrillar, oligomeric Aβ particles were present (Fig. 2). At this time-point there was no discernible ThT fluorescence at 50 μM Aβ, while 100 μM and 250 μM samples showed intermediate ThT characteristics (Fig. 1A). Additionally, after 6 h of incubation we observed numerous roughly spherical oligomeric species, which ranged from 12 to 25 nm in diameter visible in the Aβ samples (in addition to fibrils). These oligomers constituted approximately 82% and 21% of the total particle count (fibrils + oligomers) at 50 μM and 250 μM concentrations, respectively (Fig. 4). After 86 h, all tested Aβ concentrations contained large quantities of mature amyloid fibrils (Fig. 2). The Aβ fibrils at 86 h displayed different morphological characteristics from the 6 h fibrils (Fig. 4).

Examination of the mature fibrils present at different stages of the fibril formation process revealed differences in the morphological characteristics of fibrils present at early (i.e. 6 h) and later (i.e. 86 h) stages of fibril formation. At 250 μM, only 12% of the fibrils observed after 6 h of incubation were longer than 600 nm, while at 86 h the proportion of these longer fibrils increased to 31% (Fig. 4). Additionally, the width of the fibrils at the 6 h time-point were observed to be 11.1 ± 0.3 nm, which was significantly smaller than the width of the fibrils at 86 h, 15.3 ± 0.5 nm. As seen in Fig. 4, the 86 h sample also showed a broader distribution of fibril widths

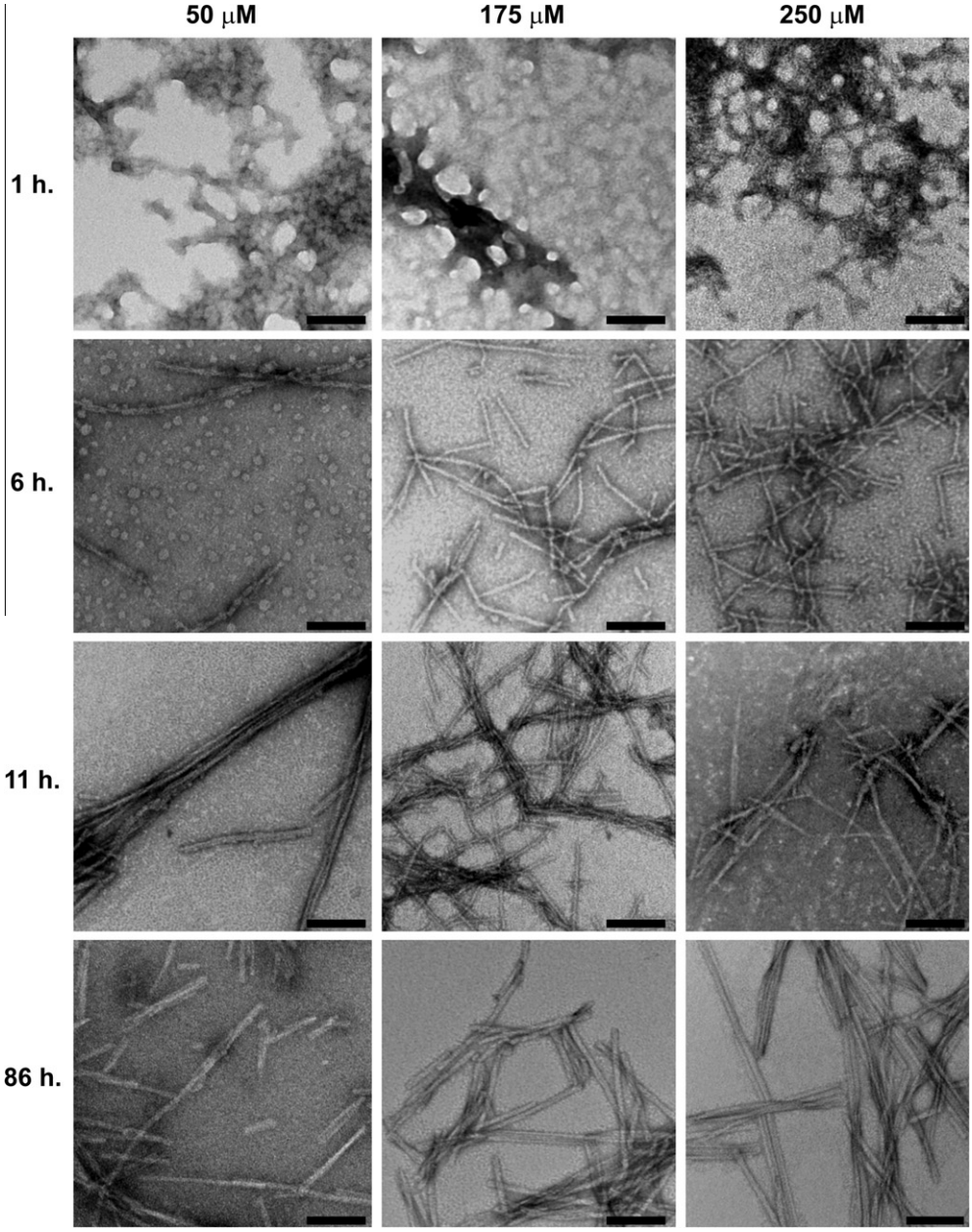

Fig. 2. TEM images on the aggregation of Aβ(1–40). Showing the 1, 6, 11 and 86 h samples. Fibril formation was in 50 mM HEPES buffer, pH 7.4 at 37 °C and the 50 μM, 175 μM and 250 μM Aβ(1-40) peptide concentrations are shown. Scale bars indicate 100 nm.

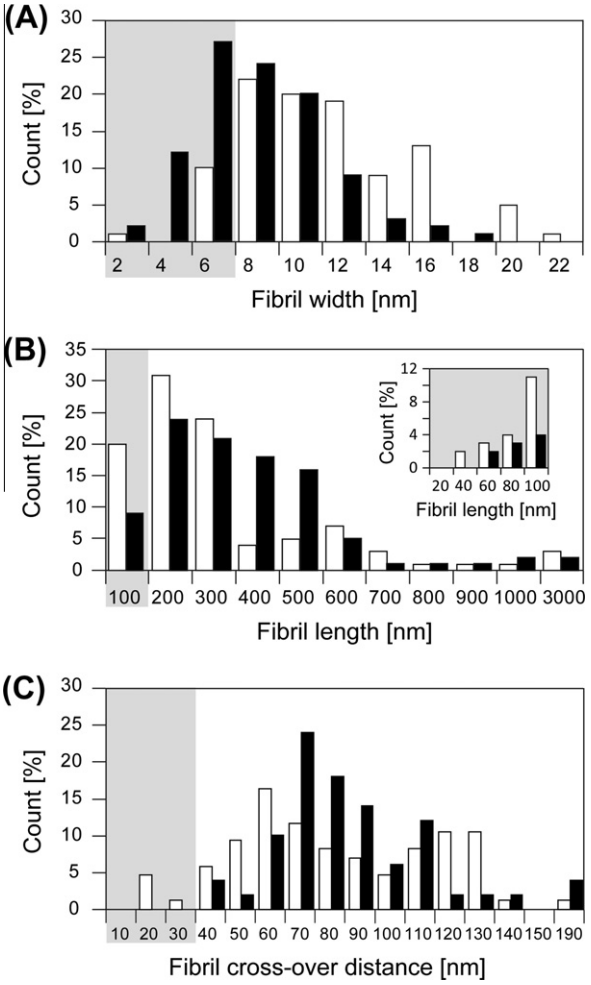

Fig. 3. Concentration-dependent morphological features of Aβ(1–40) fibrils, formed at 50 μM and 250 μM for 6 h. Counts of the fibrillar fraction of 50 μM (white bars) and 250 μM (black bars) Aβ(1–40) samples after 6 h of incubation at 37 °C. The width (A), length (B) and cross-over distance (C) of fibrillar structures are shown. Grey boxes indicate populations which show protofibril characteristics.

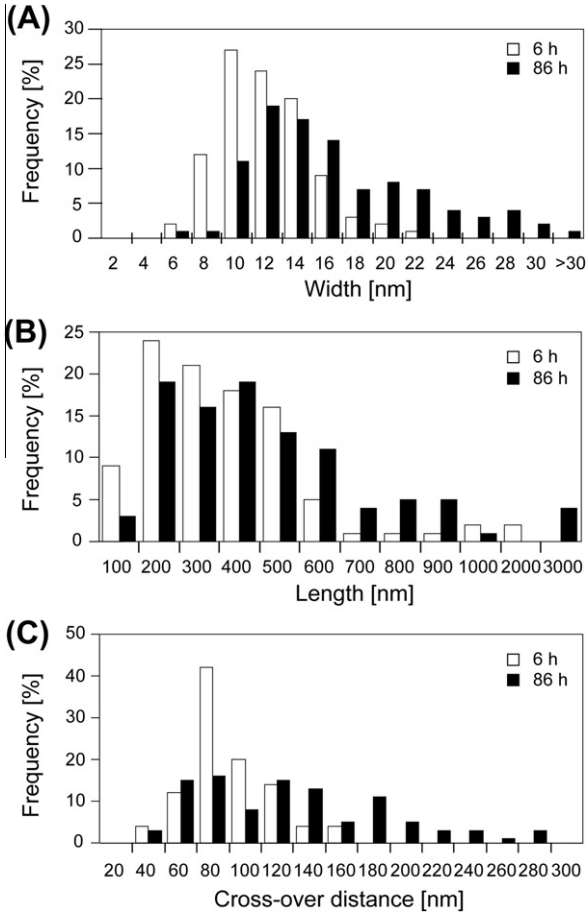

Fig. 4. Time-dependent morphological features of Aβ(1–40) fibrils, incubated at 250 μM for 6 and 86 h. Counts of the fibrillar fraction of 250 μM Aβ(1–40) incubated for 6 (white bars) and 86 (black bars) h at 37 °C. The width (A), length (B) and cross-over distance (C) of fibrillar structures are shown.

and cross-over distances (a characteristic, periodic thinning of the fibril width in a given fibril). These changes indicate an increased polymorphism of the fibril structures present at 86 h, as compared to the 6 h samples.

4. Discussion

Previous models of Aβ amyloid fibril formation have frequently focused on the importance of nucleus formation within the lag phase [2,4,10,11]. Our current data, while not in conflict with the nucleation theory *per se*, instead provides support for a larger role of secondary processes and alternating pathways within Aβ kinetics. We used a single-particle technique (EM) to show that significant quantities of mature Aβ(1–40) amyloid fibrils occur within the apparent lag phase, as defined by ThT fluorescence. This provides experimental support for the role of fibril fragmentation in inducing the growth phase and demonstrates that fibrils must have been already formed during the lag phase. This has been previously argued on primarily theoretical grounds based on data gained from bulk spectroscopic methods [3,9].

We have demonstrated the presence of intermediate species in the 250 μM Aβ fibrillation kinetics. This implies a different mechanism of fibril formation occurs here, than at low concentration (50 μM). This finding deviates from reports of other Aβ fibrillation reactions, where increasing concentration is consistently associated with more rapid fibril formation, and where no intermediate ThT step was observed within the investigated window of concentrations [4,10,11]. Importantly, these data were obtained with thoroughly disaggregated peptide, which argues against a strong influence of pre-aggregated material.

In our data, at high concentrations, the kinetic pathway features a clear intermediate ThT step. This signifies a more dominant involvement of secondary processes or competing alternative pathways, associated with either the oligomeric and/or amyloid fibril structures which are present in these samples. These unusual kinetic features, which affect both t_l and k, implies that reassembly of such structures is required. This may involve either disassembly into monomers or inter-fibril structural reassembly.

In previous studies on the fibrillation kinetics Aβ(1–40), made at lower concentrations, Aβ(1–40) demonstrates concentration dependence [10]. At the higher concentrations examined in our study, a kinetic intermediate species was apparent at around 6 h (Fig. 1A and D). These species are linked to the altered kinetic rate of the Aβ fibril formation, which is unexpectedly slowed at peptide concentrations above 100 μM. Both mature fibrils and oligomers were observed at this time-point (Fig. 2), and thus there is the potential for at least two processes to be occurring, individually or in tandem. Firstly, the oligomeric species may be slowing the kinetic rate of fibril formation. This could be due to a requirement for disassembly and reassembly of the oligomer i.e. from a non-fibril

competent oligomer back to fibril competent monomers. Non-fibril competent oligomers have been observed previously for Aβ [10] and for other amyloid forming proteins [12]. A second possibility is that structural rearrangement of the early stage fibrils is required for them to progress to late stage fibrils. Alterations in fibril width and cross-over distance are indicative of large scale structural rearrangement, wherein the Aβ fibrils are featuring different numbers or internal alignment of the protofilaments [13]. Such alterations have been observed for other amyloid forming proteins [14] and could conceivably result in the fluctuations in ThT fluorescence observed over the initial 24 h period for Aβ samples at 100 μM and above (Fig. 1A).

By investigating the fibrillation kinetics of Aβ(1–40) at higher concentrations, we have established that there is a limit to this peptide's apparent concentration dependent qualities. Instead, at high peptide concentrations secondary processes supersede the conventional folding kinetics of this peptide. Further work will establish if these concentration effects are also applicable to Aβ(1–42) and how they may affect the interactions between these two peptides.

In conclusion, Aβ(1–40) fibrillation kinetics do not always follow conventional kinetic mechanisms. Instead, at high concentrations, intermediate structures are present and secondary processes further dictate the speed of fibrillation.

Acknowledgments

The authors would like to thank Prof. Fändrich for his invaluable guidance and assistance. MG would like to thank W.F. Xue for discussions on concentration kinetic analysis.

References

[1] R. Wetzel, Kinetics and thermodynamics of amyloid fibril assembly, Acc. Chem. Res. 39 (2006) 671–679.
[2] J.D. Harper, P.T. Lansbury Jr., Models of amyloid seeding in Alzheimer's disease and scrapie: mechanistic truths and physiological consequences of the time-dependent solubility of amyloid proteins, Annu. Rev. Biochem. 66 (1997) 385–407.
[3] T.P. Knowles, C.A. Waudby, G.L. Devlin, S.I. Cohen, A. Aguzzi, M. Vendruscolo, E.M. Terentjev, M.E. Welland, C.M. Dobson, An analytical solution to the kinetics of breakable filament assembly, Science 326 (2009) 1533–1537.
[4] D.M. Walsh, A. Lomakin, G.B. Benedek, M.M. Condron, D.B. Teplow, Amyloid beta-protein fibrillogenesis. Detection of a protofibrillar intermediate, J. Biol. Chem. 272 (1997) 22364–22372.
[5] C.S. Goldsbury, S. Wirtz, S.A. Muller, S. Sunderji, P. Wicki, U. Aebi, P. Frey, Studies on the in vitro assembly of a beta 1–40: implications for the search for a beta fibril formation inhibitors, J. Struct. Biol. 130 (2000) 217–231.
[6] M. Garvey, K. Tepper, C. Haupt, U. Knupfer, K. Klement, J. Meinhardt, U. Horn, J. Balbach, M. Fandrich, Phosphate and HEPES buffers potently affect the fibrillation and oligomerization mechanism of Alzheimer's Aβ peptide, Biochem. Biophys. Res. Commun. 409 (2011) 385–388.
[7] P. Hortschansky, V. Schroeckh, T. Christopeit, G. Zandomeneghi, M. Fandrich, The aggregation kinetics of Alzheimer's beta-amyloid peptide is controlled by stochastic nucleation, Protein Sci. 14 (2005) 1753–1759.
[8] F. Chiti, N. Taddei, F. Baroni, C. Capanni, M. Stefani, G. Ramponi, C.M. Dobson, Kinetic partitioning of protein folding and aggregation, Nat. Struct. Biol. 9 (2002) 137–143.
[9] W.-F. Xue, S.W. Homans, S.E. Radford, Systematic analysis of nucleation-dependent polymerization reveals new insights into the mechanism of amyloid self-assembly, Proc. Natl. Acad. Sci. USA 105 (2008) 8926–8931.
[10] T.H.J. Huang, D.-S. Yang, P.E. Fraser, A. Chakrabartty, Alternate aggregation pathways of the Alzheimer beta-amyloid peptide: an in vitro model of preamyloid, J. Biol. Chem. 275 (2000) 36436–36440.
[11] M.-S. Lin, L.-Y. Chen, H.-T. Tsai, S.S.S. Wang, Y. Chang, A. Higuchi, W.-Y. Chen, Investigation of the mechanism of beta-amyloid fibril formation by kinetic and thermodynamic analyses, Langmuir 24 (2008) 5802–5808.
[12] S.B. Padrick, A.D. Miranker, Islet amyloid: phase partitioning and secondary nucleation are central to the mechanism of fibrillogenesis, Biochemistry 41 (2002) 4694–4703.
[13] J. Meinhardt, C. Sachse, P. Hortschansky, N. Grigorieff, M. Fändrich, A beta(1–40) fibril polymorphism implies diverse interaction patterns in amyloid fibrils, J. Mol. Biol. 386 (2009) 869–877.
[14] J.S. Pedersen, D. Dikov, J.L. Flink, H.A. Hjuler, G. Christiansen, D.E. Otzen, The changing face of glucagon fibrillation: structural polymorphism and conformational imprinting, J. Mol. Biol. 355 (2006) 501–523.